Supporting information for "Linking future precipitation changes to weather features in CESM2-LE"

Kjersti Konstali[1], Thomas Spengler[1], Clemens Spensberger[1], Asgeir Sorteberg [1]

[1]Geophysical Institute, University of Bergen, and Bjerknes Centre for Climate Research, Bergen, Norway

Contents of this file

Text S1. Feature climatology

The qualitative pattern of cyclone occurrences is very similar to ERA5 (Figure S2a,b and Figure S3a,b). The cyclone frequency maximizes along the North Atlantic, North Pacific and Southern Ocean storm track. The overestimation in North Atlantic DJF (Figure S2a,b) co-occurs with the location of the maximum total precipitation, located just south of Iceland (Figure 1a,b). CESM2 has slightly too many cyclone occurrences compared to ERA5, particularly poleward of 60°. In the North Atlantic poleward of 60°, the cyclones occur up to 10% more often in CESM2 than in ERA5 in DJF, whereas the frequency is more than 5% higher in the Southern Ocean poleward of 60°S in JJA.

However, the bias in cyclone occurrences does not resemble the stormtrack bias in (Priestley et al., 2020), where the NH stormtracks are located too far equatorward. Instead, CESM2 shows too many cyclones in the polar regions. Some of the differences can most likely be ascribed to the difference in detection methods, as (Priestley et al., 2020) detects cyclone using vorticity at 850 hPa, while we use mean sea level pressure and consider the area of the cyclone.

Like cyclones, fronts mark the location of the major stormtracks in both hemispheres (Figure S2c,d and Figure S3c,d). In addition, some fronts are detected in the subtropical regions, such as over the equatorial Atlantic and in the Indian Ocean. The subtropical fronts are most likely related to moisture gradients rather than temperature gradients.

The frequency of fronts is overestimated in both hemispheres, with similar biases as the cyclone frequency (Figure S2a,b and Figure S3a,b). There are too many fronts in the high latitudes (between 5-10% in DJF and JJA in both hemispheres), but the maximum bias tends to be slightly offset to the equatorward side of the maximum bias in the cyclones. This shift in location of bias between cyclones and fronts is consistent with occurrences of trailing cold fronts associated with the cyclones. The difference is larger in the summer hemisphere than in the winter hemisphere, indicating that some of the bias is most likely due to the moisture gradient. Some of the differences may also be associated with the difference in the detection method. As the fronts in ERA5 are detected using three levels, these fronts likely affect a deeper layer of the atmosphere. However, as we chose a relatively higher threshold for the detection in ERA5, we may have counteracted some of this effect.

MTAs also frequently occur along the stormtracks (Figure S2e,f and Figure S3e,f), as they represent atmospheric rivers which are the result of moisture convergence along the cold front (Dacre et al., 2015). The frequency of MTAs is slightly underestimated over the stormtrack regions (0-3% in NH in DJF), while it is slightly overestimated downstream (5-7% over Europe in DJF). In addition, the intertropical convergence zone (ITCZ) and the monsoon circulations are picked up as MTAs (Konstali et al., 2024; Spensberger et al., 2024). MTAs also detect low-level jets (LLJ), such as the Great Plains LLJ and the South American LLJ. However, these jets are less clearly defined in CESM2 than in ERA5. The South American LLJ emerges from the edge of the Amazon rather than being a continuous feature which transports moisture from the Gulf of Mexico to the La Plata Basin, as in ERA5 in DJF (Figure S2e,f). Similarly, the Great Plains LLJ is less clearly defined, indicating that the moisture transport from the Gulf of Mexico to the Great Plains is weaker or without a clearly defined maximum, both in DJF and JJA.

CAOs form as dry, cold air is advected from the continents or from the sea ice over a relatively warmer ocean. This leads to atmospheric convection and subsequent precipitation (i.e., Papritz & Sodemann, 2018). CAOs are present in the winter hemisphere, with the largest frequency over the Western Boundary Currents and along the sea ice edge (Figure S2g,h and Figure S3g,h).

There are larger biases associated with CAOs than the other features. In DJF, there are large biases in both the North Pacific and in the North Atlantic (Figure S2g,h). Even though the frequency is overestimated in CESM2, the frequency of occurrence is slightly lower both over Kuroshio and the Gulf Stream, while it is overestimated south of Iceland and in the Northwest Pacific. In JJA, there are no CAOs in NH, but the frequency is

overestimated in the SH (Figure S3g,h). That CAOs are less well represented is most likely due to the SST biases in CESM2 (Danabasoglu et al., 2020). The CAO frequency bias coincides with the warm SST bias (Danabasoglu et al., 2020) and as CAOs are defined where the difference between 850 hPa and the SST exceeds 3K, the frequency of CAOs is highly sensitive to the SST.

References

Dacre, H. F., Clark, P. A., Martinez-Alvarado, O., Stringer, M. A., & Lavers, D. A. (2015, aug). How Do Atmospheric Rivers Form? *Bulletin of the American Meteorological Society*, *96*(8), 1243–1255. Retrieved from https://journals.ametsoc.org/view/journals/bams/96/8/bams-d-14-00031.1.xmlhttps://journals.ametsoc.org/doi/10.1175/BAMS-D-14-00031.1 doi: 10.1175/BAMS-D-14-00031.1

Danabasoglu, G., Lamarque, J. F., Bacmeister, J., Bailey, D. A., DuVivier, A. K., Edwards, J., ... Strand, W. G. (2020). The Community Earth System Model Version 2 (CESM2). *Journal of Advances in Modeling Earth Systems*, *12*(2), 1–35. doi: 10.1029/2019MS001916

Konstali, K., Spensberger, C., Spengler, T., & Sorteberg, A. (2024). Global attribution of precipitation to weather features. *Journal of Climate*, *37*(4), 1181 - 1196. Retrieved from https://journals.ametsoc.org/view/journals/clim/37/4/JCLI-D-23-0293.1.xml doi: 10.1175/JCLI-D-23-0293.1

Papritz, L., & Sodemann, H. (2018, nov). Characterizing the local and intense water cycle during a cold air outbreak in the Nordic seas. *Monthly Weather Review*, *146*(11), 3567–3588. Retrieved from http://journals.ametsoc.org/doi/10.1175/MWR-D-18-0172.1 doi: 10.1175/MWR-D-18-0172.1

Priestley, M. D. K., Ackerley, D., Catto, J. L., Hodges, K. I., McDonald, R. E., & Lee, R. W. (2020). An overview of the extratropical storm tracks in cmip6 historical simulations. *Journal of Climate*, *33*(15), 6315 - 6343. Retrieved from https://journals.ametsoc.org/view/journals/clim/33/15/JCLI-D-19-0928.1.xml doi: https://doi.org/10.1175/JCLI-D-19-0928.1

Spensberger, C., Konstali, K., & Spengler, T. (2024, March). *Moisture transport axes: a unifying definition for monsoon air streams, atmospheric rivers, and warm moist intrusions.* Retrieved from http://dx.doi.org/10.22541/essoar.170957480.06815908/v1 doi: 10.22541/essoar.170957480.06815908/v1

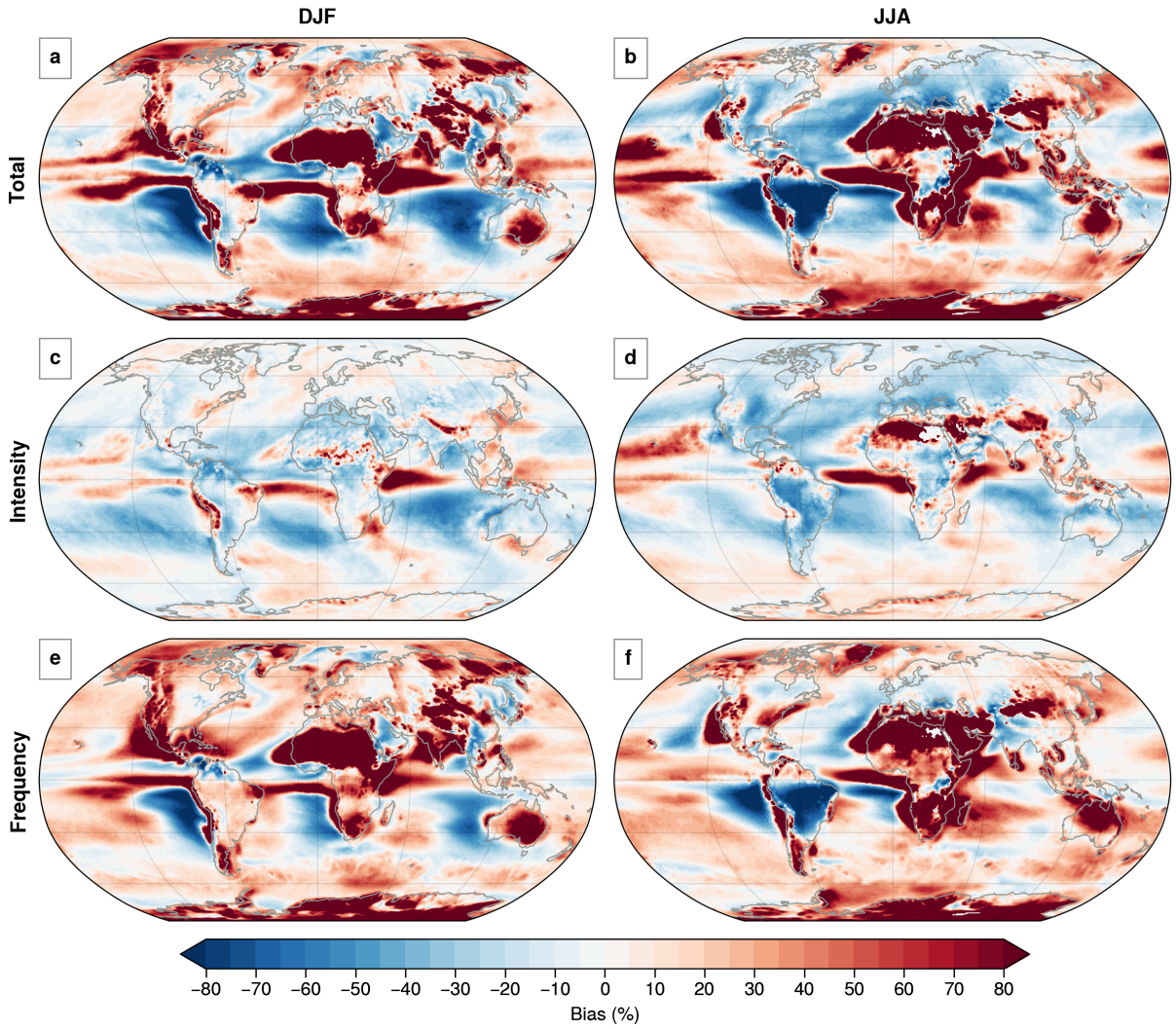

Figure S1. Precipitation bias for CESM2-LE minus ERA5 in percent with respect to ERA5 as reference for DJF (left) and JJA (right) for total precipitation (a,b), intensity (c,d) and frequency (e,f). Note that ERA5 is interpolated to the grid of CESM2 to calculate the difference.

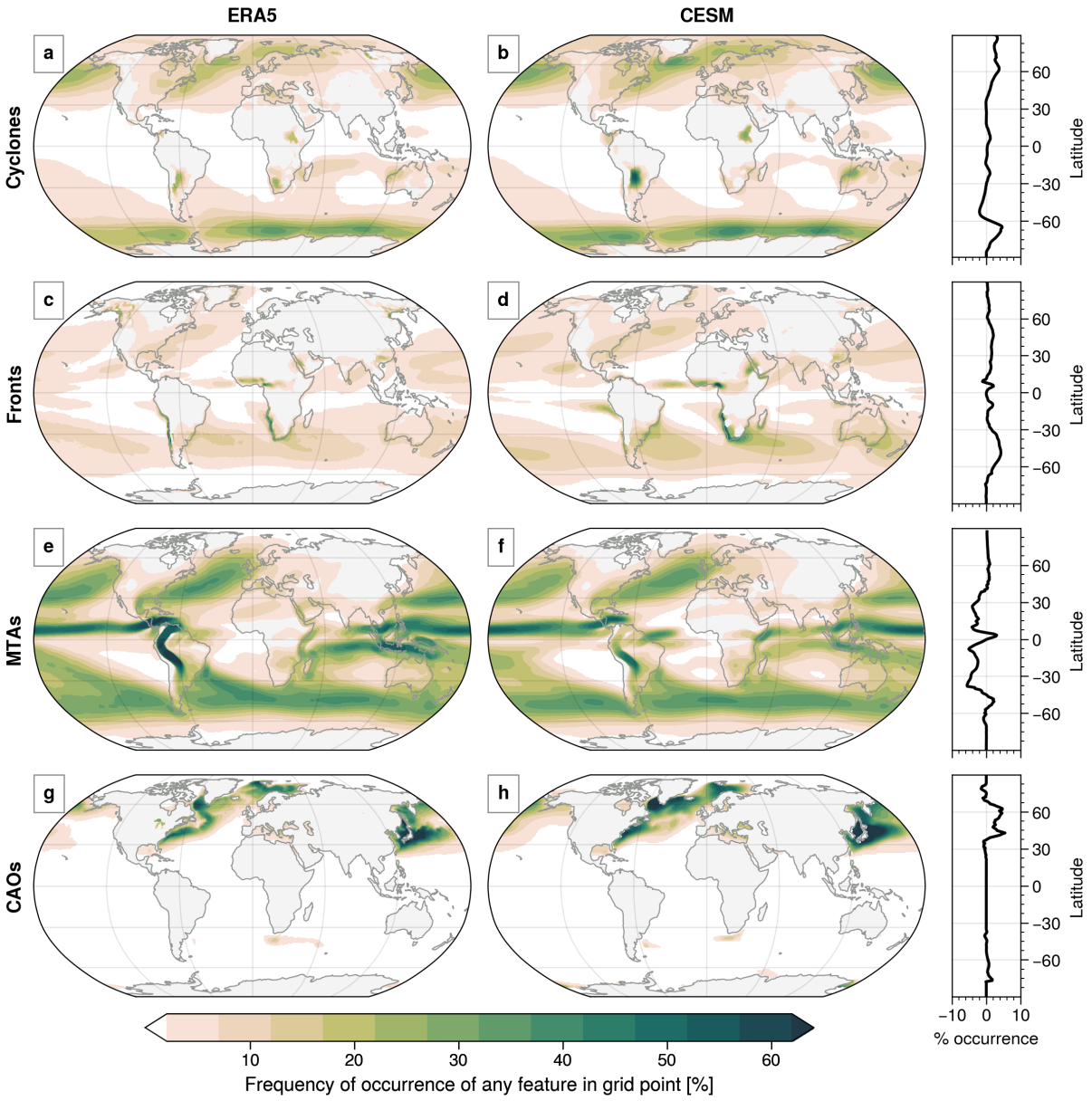

Figure S2. Comparison of ERA5 to CESM in DJF in terms of weather features. ETCs (a,b), fronts (c,d), MTAs (e,f) and CAOs (g,h). The zonal mean difference between the frequency of features between CESM and ERA5 is shown in the panels on the right.

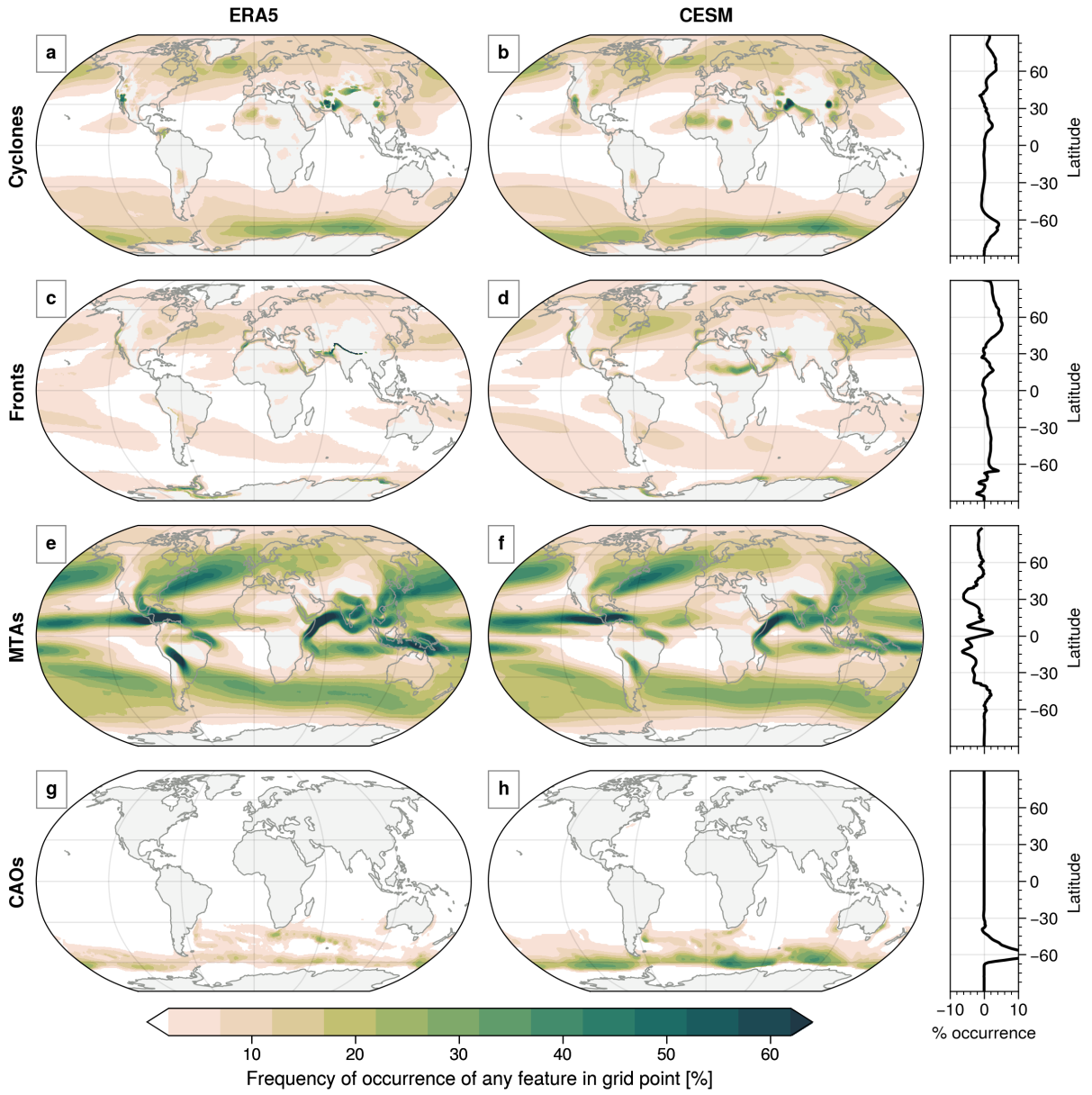

Figure S3. As Figure S2, but for JJA.

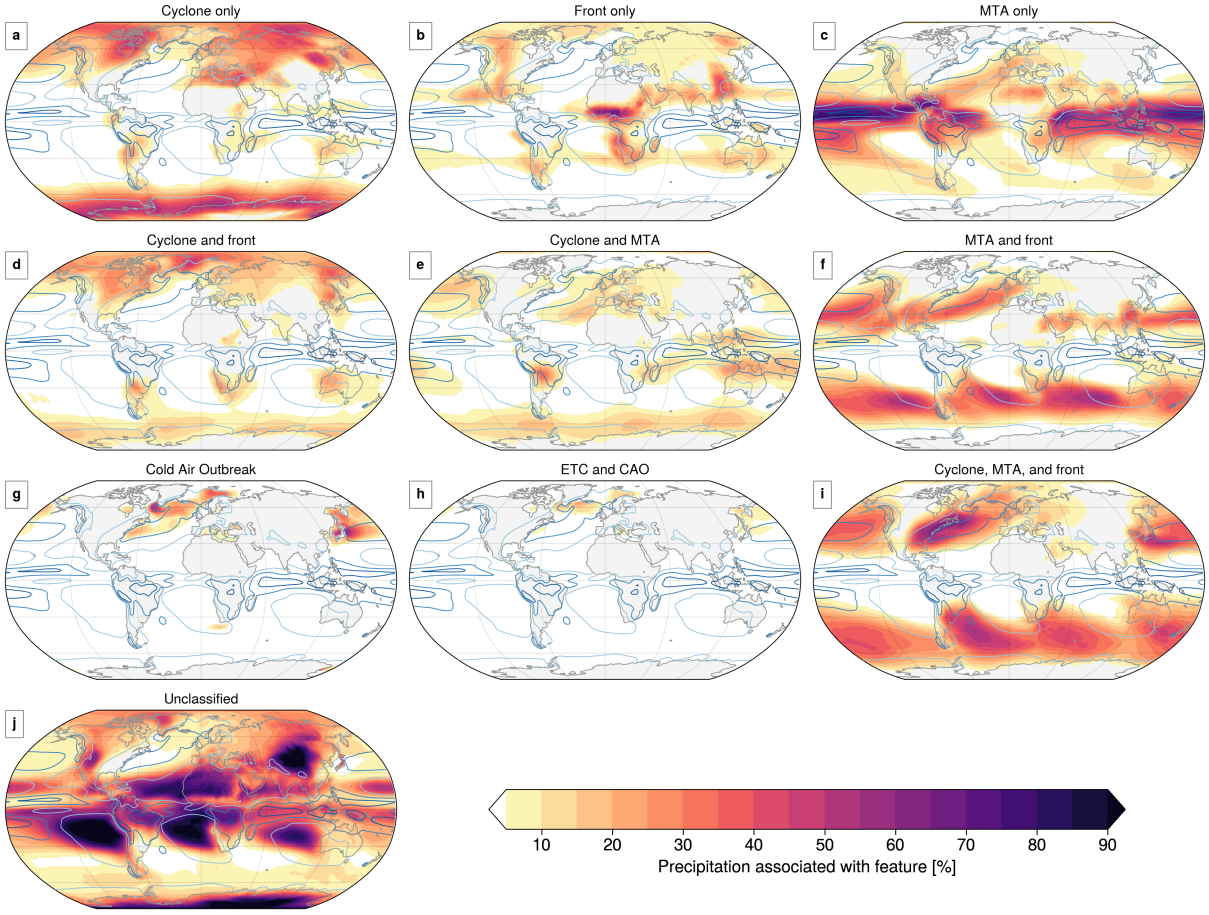

Figure S4. Contribution from the different weather features to the total precipitation in DJF over the historical period (1979-2014). The differences between seasons are small, so we show only DJF. Contours mark 50, 150, and 300 mm/month, from light to dark blue.

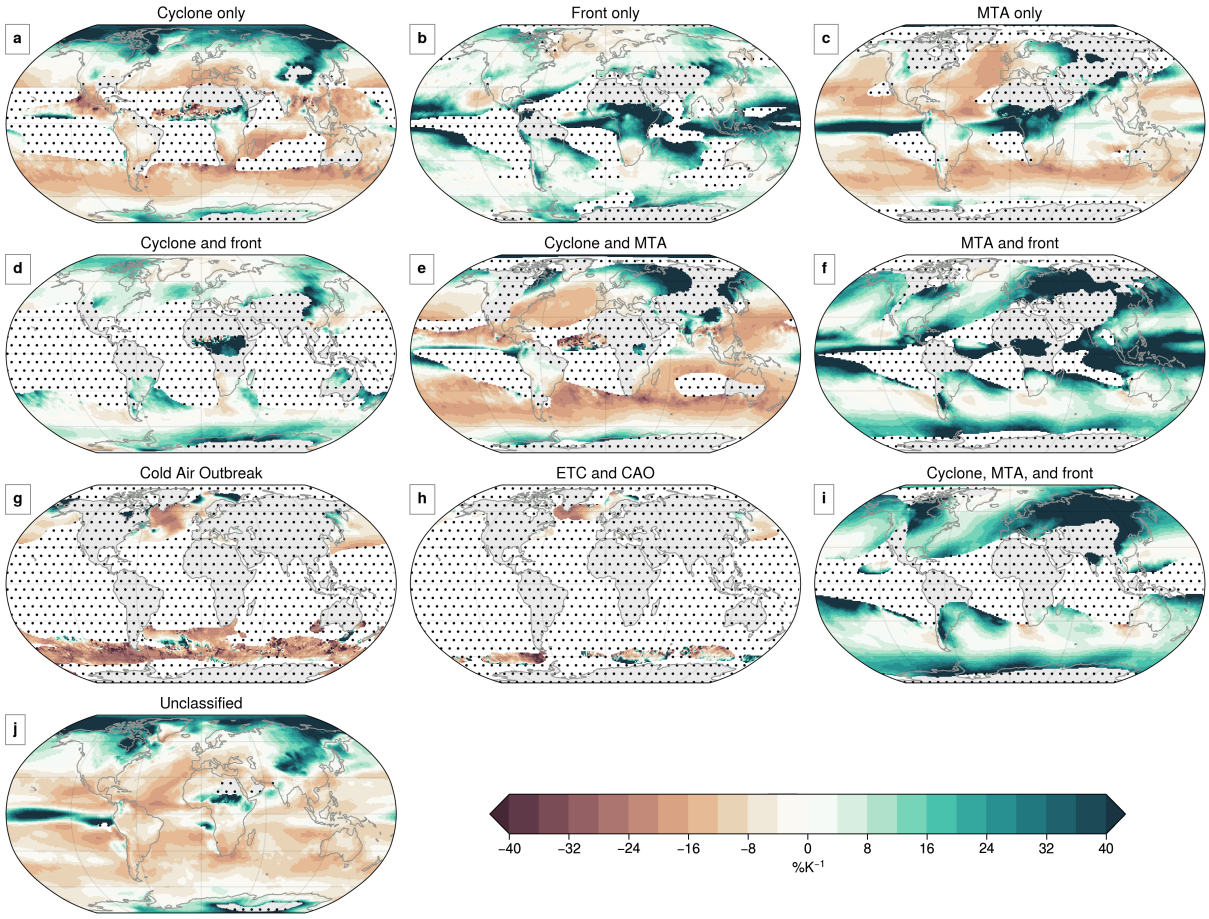

Figure S5. Relative changes in the precipitation for the different weather features in DJF. Dotted areas mark where the precipitation frequency of the respective category is less than 1.5% of the time.

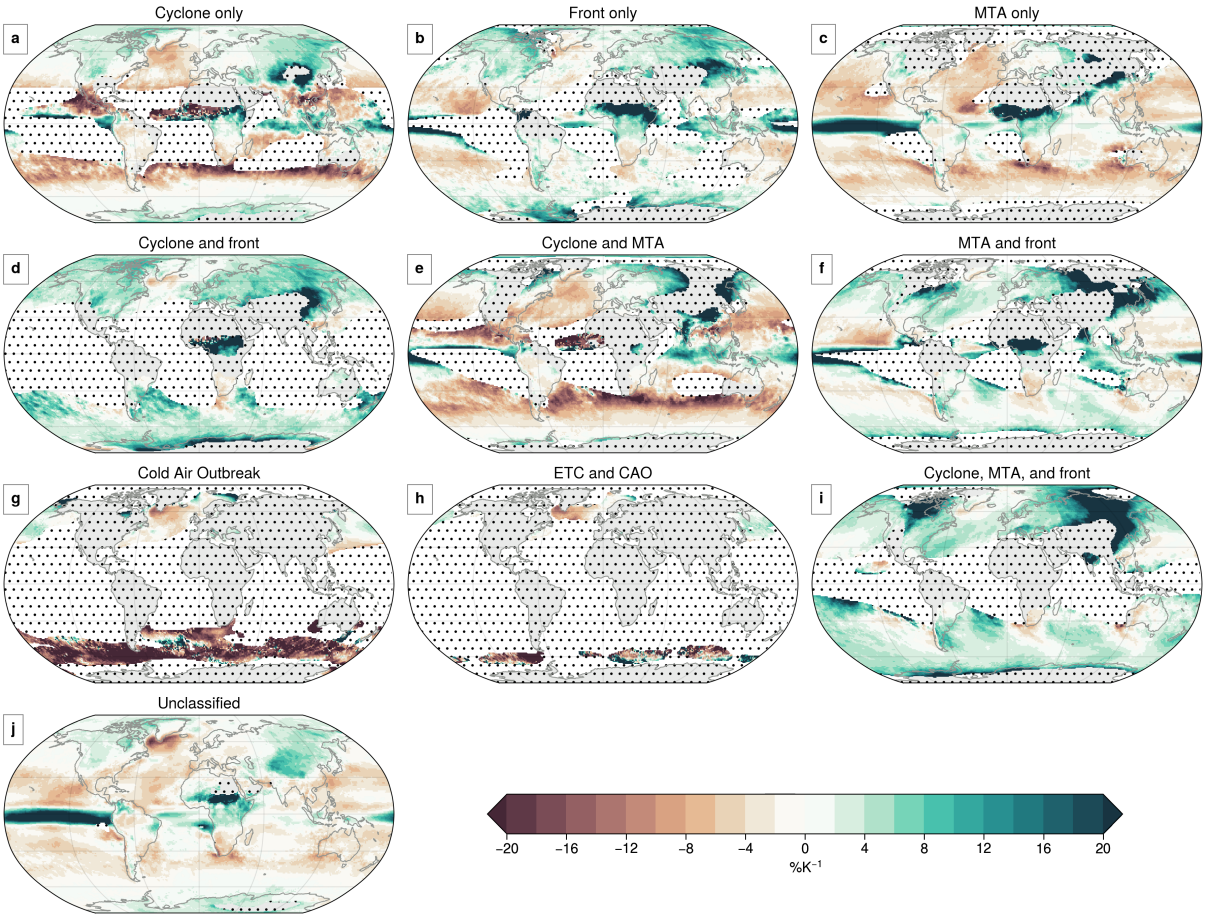

Figure S6. Relative changes in intensity (and note that the relative changes in intensity + frequency equals the total change).

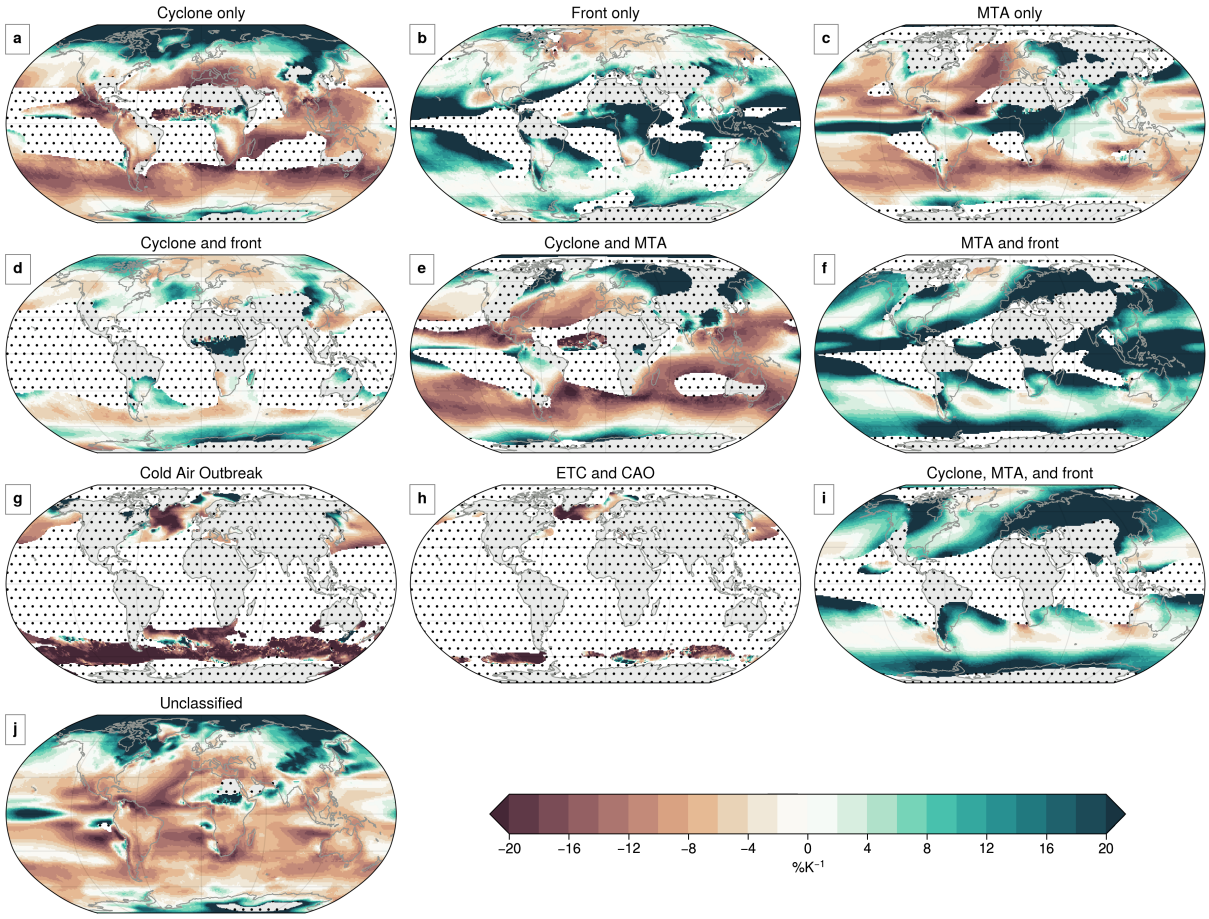

Figure S7. Same as Figure S6, but for frequency

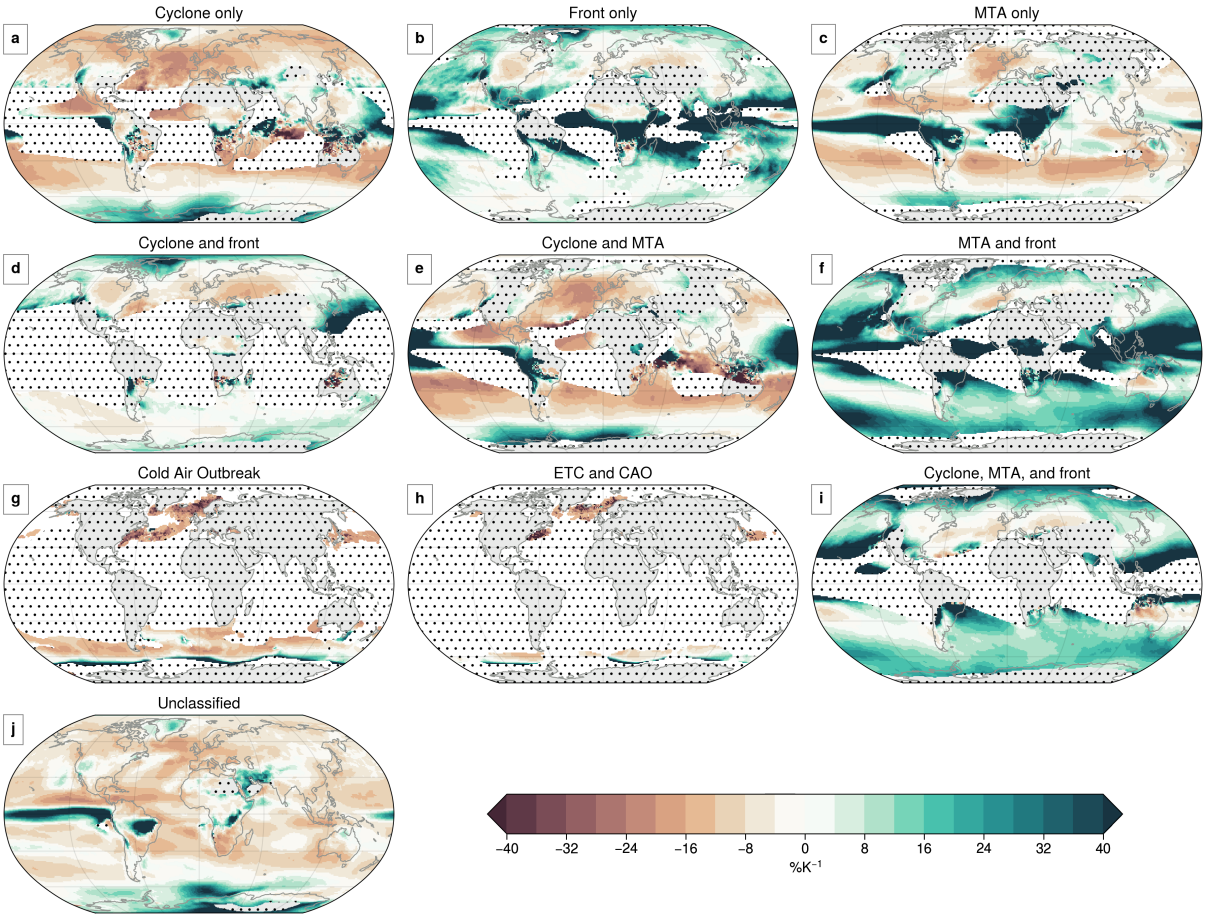

Figure S8. As in Figure S5 but for JJA

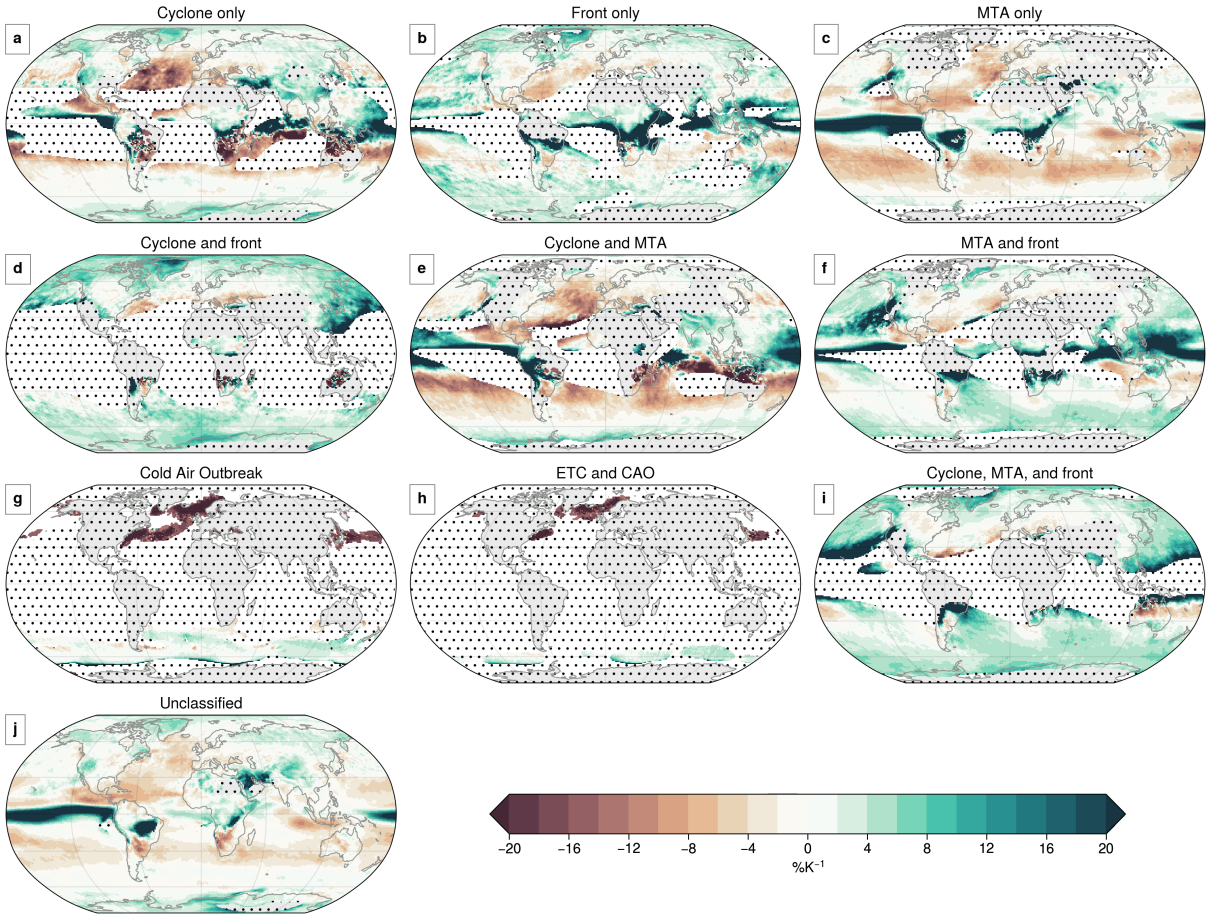

Figure S9. Same as Figure S6, but for JJA

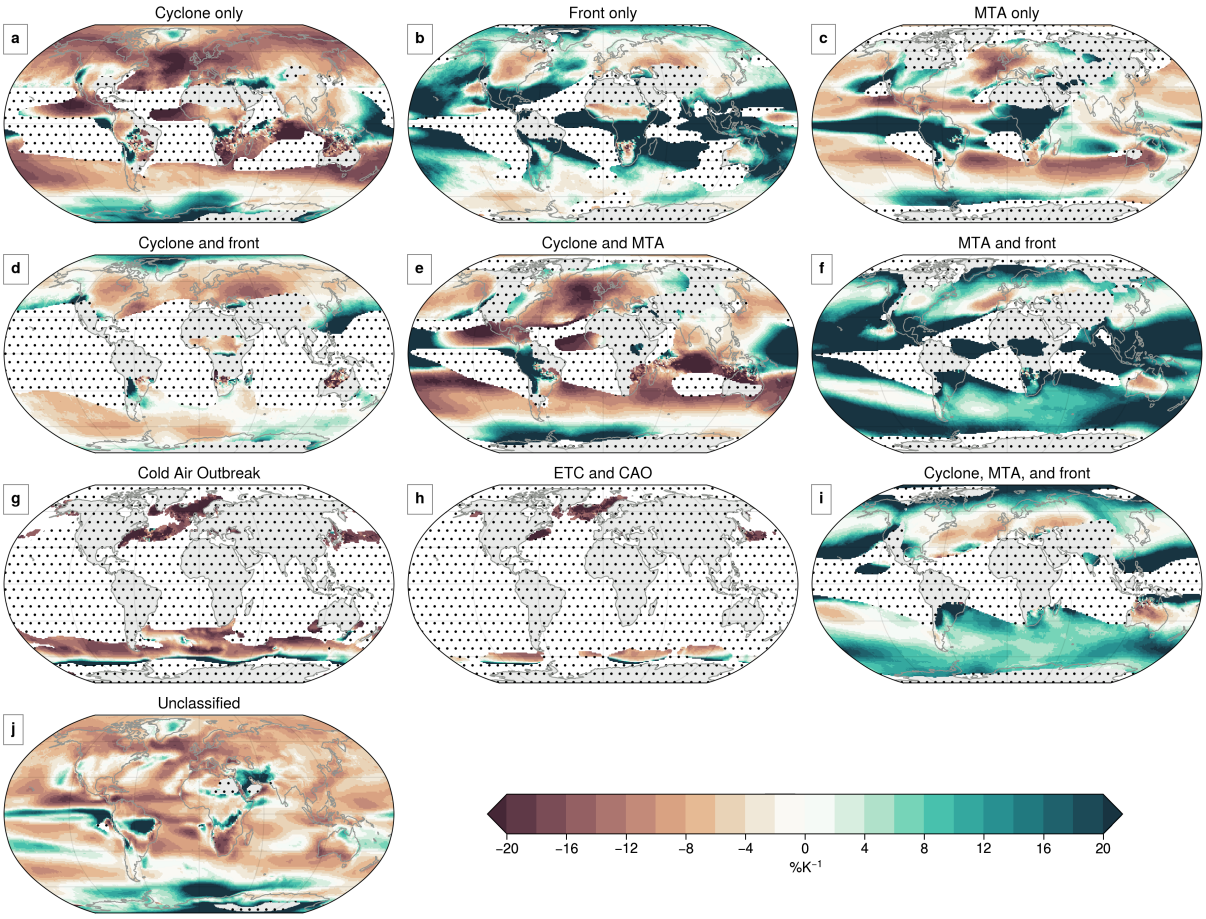

Figure S10. Same as Figure S7, but for JJA